Journal of Power Sources 229 (2013) 141–148

Contents lists available at SciVerse ScienceDirect

Journal of Power Sources

journal homepage: www.elsevier.com/locate/jpowsour

Density functional molecular dynamics simulations investigation of proton transfer and inter-molecular reorientation under external electrostatic field perturbation: Case studies for water and imidazole systems

Piyarat Nimmanpipug [a,b,*], Janchai Yana [a,b,c], Vannajan Sanghiran Lee [a,b,d], Sornthep Vannarat [e], Suwabun Chirachanchai [f], Kohji Tashiro [g,**]

[a] Computational Simulation and Modeling Laboratory (CSML), Department of Chemistry and Center for Innovation in Chemistry, Faculty of Science, Chiang Mai University, Chiang Mai 50200, Thailand
[b] Thailand Center of Excellence in Physics (ThEP), Commission on Higher Education, Bangkok 10400, Thailand
[c] Department of Chemistry, Faculty of Science and Technology, Chiang Mai Rajabhat University, Chiang Mai 50300, Thailand
[d] Department of Chemistry, Faculty of Science, University of Malaya, Kuala Lumpur 50603, Malaysia
[e] Large Scale Simulation Research Laboratory, National Electronics and Computer Technology Center, Pathumthani 12120, Thailand
[f] The Petroleum and Petrochemical College, Chulalongkorn University, Bangkok 10330, Thailand
[g] Department of Future Industry-Oriented Basic Science and Materials, Graduate School of Engineering, Toyota Technological Institute, Nagoya 468-8511, Japan

HIGHLIGHTS

- A relationship between packing structure and proton conductivity was carried out.
- Proton movement was analysed in DFT-MD simulation with electric field perturbation.
- Reorientation and tilted proton hopping direction were found in imidazole crystal.

ARTICLE INFO

Article history:
Received 4 September 2012
Received in revised form
29 November 2012
Accepted 3 December 2012
Available online 12 December 2012

Keywords:
Density functional molecular dynamics simulations
Proton transfer
Electrostatic field perturbation
Imidazole

ABSTRACT

Proton transfer is a governing factor in the proton exchange efficiency in membrane fuel cells (PEMFCs), which are an alternative environmentally friendly resource. To develop the capacity of the PEMFC system, anhydrous membranes containing imidazole groups have garnered much interest. In this research, the relationship between the hydrogen bond networks, including the consequent packing structure, and the proton conductivity of water and imidazole (Im) systems have been systematically studied. The effect of external electrostatic perturbation was investigated in $(H_2O)H^+\cdots H_2O$, $(Im)H^+\cdots Im$, bulk water, and imidazole superlattice systems. In all of these cases, the application of an electric field in a direction opposite to that of the overall system dipole significantly reduces the activation barrier for proton transport. In isolated systems, $(H_2O)H^+\cdots H_2O$ and $(Im)H^+\cdots Im$, the preferred orientation angle between the neighbouring molecules was 90°. From density functional molecular dynamics simulations of the bulk system, the proton diffusion coefficient was found to increase under the perturbation by the applied electric fields in range of 1.29×10^7 to 3.86×10^7 V cm^{-1} (0.0025–0.0075 a.u.) for both water and imidazole. To trace the efficient proton transfer, the proton movement trajectory was explicitly analysed in detail. Interestingly, a tilted proton hopping direction was found for imidazole crystal.

1. Introduction

Water is essential for proton transfer in Nafion or sulfonated fluorine polymer, allowing these materials to function as electrolytic polymers. Because of the higher rate of water evaporation at high temperature, Nafion has a limited working temperature range to induce an enormous reduction of proton conductivity: the

* Corresponding author. Thailand Center of Excellence in Physics (ThEP), Commission on Higher Education, Bangkok 10400, Thailand. Tel.: +66 53943341x136; fax: +66 892277.
** Corresponding author.
E-mail addresses: piyaratn@gmail.com (P. Nimmanpipug), ktashiro@toyota-ti.ac.jp (K. Tashiro).

0378-7753/$ – see front matter © 2012 Elsevier B.V. All rights reserved.
http://dx.doi.org/10.1016/j.jpowsour.2012.12.012

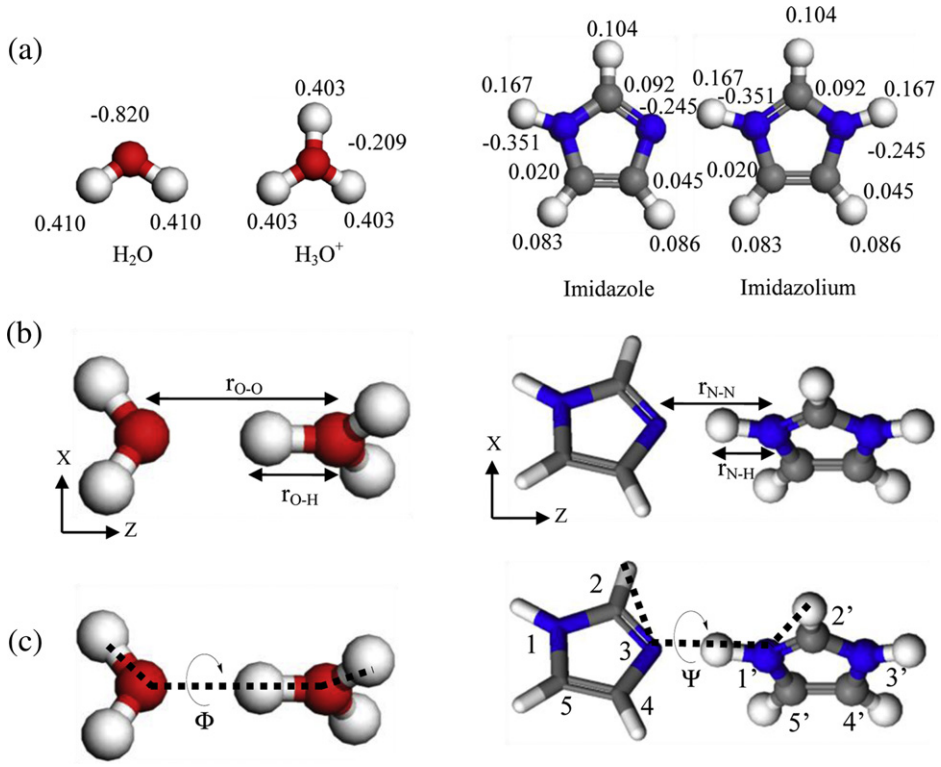

Fig. 1. (a) Structures of the optimised water, H_3O^+, optimised (Im), and imidazolium ion (ImH^+) models. (b) The initial structure of the $(H_2O)H^+\cdots H_2O$ and $(Im)H^+\cdots Im$ models. (c) The inter-molecular torsional angles: Φ for the $(H_2O)H^+\cdots H_2O$ system and Ψ for the $(Im)H^+\cdots Im$ (Ψ) system.

conductivity at high temperature (80 °C) is more than ten-fold lower than that at lower temperature (60 °C) [1–6]. In addition to membrane dehydration and the reduction of ionic conductivity, Nafion exhibited a loss of mechanical strength due to the softening of the polymer backbone and increased parasitic losses through high fuel permeation at temperatures above 80 °C [1,5]. There are several approaches to overcoming these problems, including the addition of a composite material to protect the water molecules at high temperature [4,5] and the development of a new water-free proton-conducting membrane [6–13].

Imidazole-based polymers have been developed as water-free proton-conducting membranes [6–13]. Imidazole itself can act as the proton solvent and the protonic charge carriers in fuel cell membranes [6–8]. Many studies have indicated that imidazole can increase the proton conductivity of the proton transfer between immobilised heterocycles via proton hopping (Grotthuss-type mechanism) [6,9,10]. This process is generally very complex, requiring the thermally activated accessibility of quite different configurations, such as very short or elongated hydrogen bonds [6,8–11].

There are number of theoretical studies of proton transfer mechanism in the imidazole system [13–25]. For example, fluorinated imidazoles were studied as proton carriers for water-free fuel cell membranes by Deng et al. [13] to investigate the poisoning of platinum (Pt) in the imidazole atmosphere. The structures of imidazole (Im) and trifluoroimidazole (ImF) were optimised by molecular dynamics (MD) simulation, and the proton-transfer hopping barrier was calculated using the B3LYP/6-311G**++ level of theory [14–17]. According to their results, with an increase in the N–N distance, the activation barrier for proton transfer increased sharply. At a certain (short) N–N distance, the proton transfer

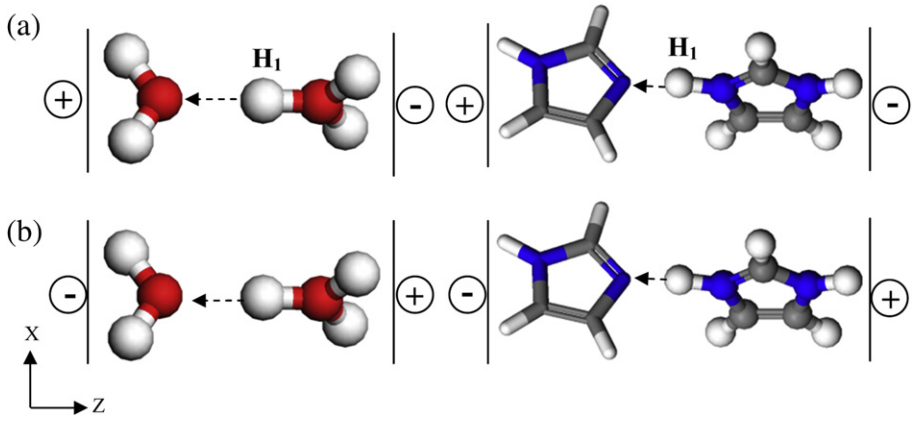

Fig. 2. Proton transfer direction with (a) positive and (b) negative applied electric fields.

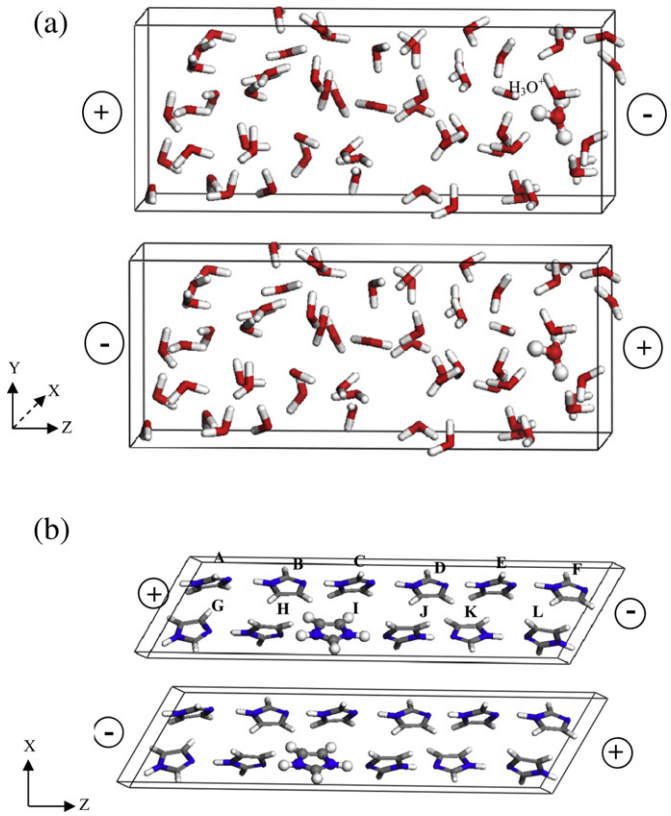

Fig. 3. Initial structure of (a) water in the bulk phase and (b) the imidazole superlattice system with positive (above) and negative (below) applied electric fields along the *Z* axis.

occurred without any barrier. This situation suggests that a polymer system with imidazole units in successive arrays should enhance proton conductivity due to the smaller N–N distance between imidazole rings.

The concept of a rotational potential energy surface (PES) was used to show the rotation barrier of imidazole, phosphoric acid, and sulfonic acid bearing alkyl molecules in a study by Paddison et al. [18]. The rotational barriers of imidazole, phosphoric acid, and sulfonic acid were calculated to be 3.9, 10.0, and 15.9 kJ mol^{-1}, respectively. The binding energy of 2-methyl imidazole and a water molecule was lower than those of phosphoric acid and sulfonic acid with a water molecule. From the study by Paddison et al., imidazole linked with an alkyl chain can move flexibly, and the water retained in the model showed the imidazole is more hydrophobic than oxo-acids. To study the effect of such fluctuation through the reorientation, Car–Parrinello molecular dynamics (CPMD) simulations were employed [19,21,24]. The studies suggested that the suitable simulation time and time step should be in ranges of 1–10 ps and 0.1–1 fs, respectively. Münch et al. [19] studied the imidazole crystal system consisting of two repeating units along the *c* axis [20] for the CPMD simulation. They found that the use of a 6 ps simulation time is sufficient for the configurations of the imidazole transition and protonic defect neighbourhood in the mechanism. The configuration showed the significant impact of these properties on proton transfer. However, they suggested that the simulation time was too short to observe a successful reorientation step. As noted by Iannuzzi et al. [21], the diffusion process cannot be observed by an *ab initio* MD simulation spanning a short time because of the high energy barriers. They developed a metadynamics (MTD) technique [21–24], which allows large barriers to be overcome in a short simulation time, i.e., a few picoseconds. Iannuzzi et al. [21] studied proton transfer in heterocyclic crystals using the MTD technique. In the MTD simulation, a migration of a charge defect over four molecules forming a chain in less than 15 ps of simulation time was observed. In addition, this dynamic trajectory indicated a complex diffusion pathway with molecular reorientation.

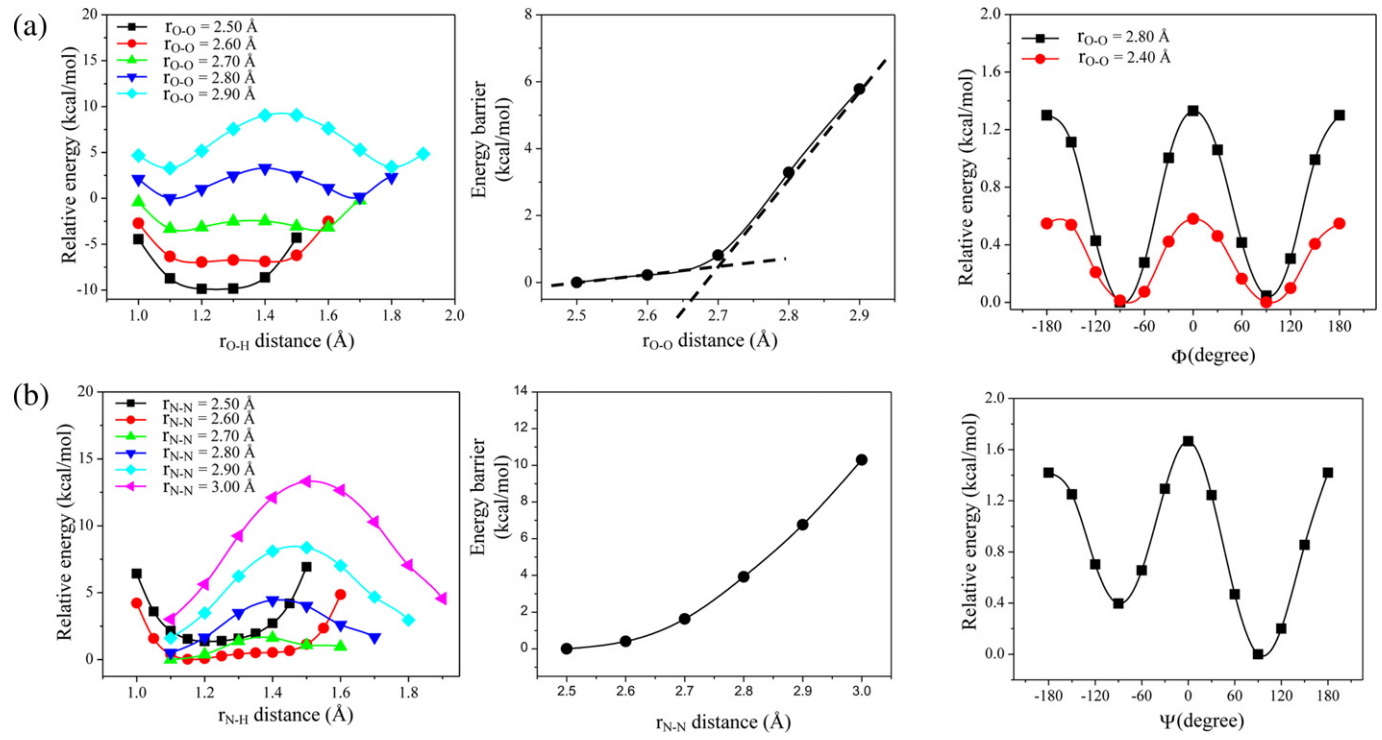

Fig. 4. Energy profile change of the proton hopping of the (a) $(H_2O)H^+\cdots H_2O$ and (b) $(Im)H^+\cdots Im$ systems.

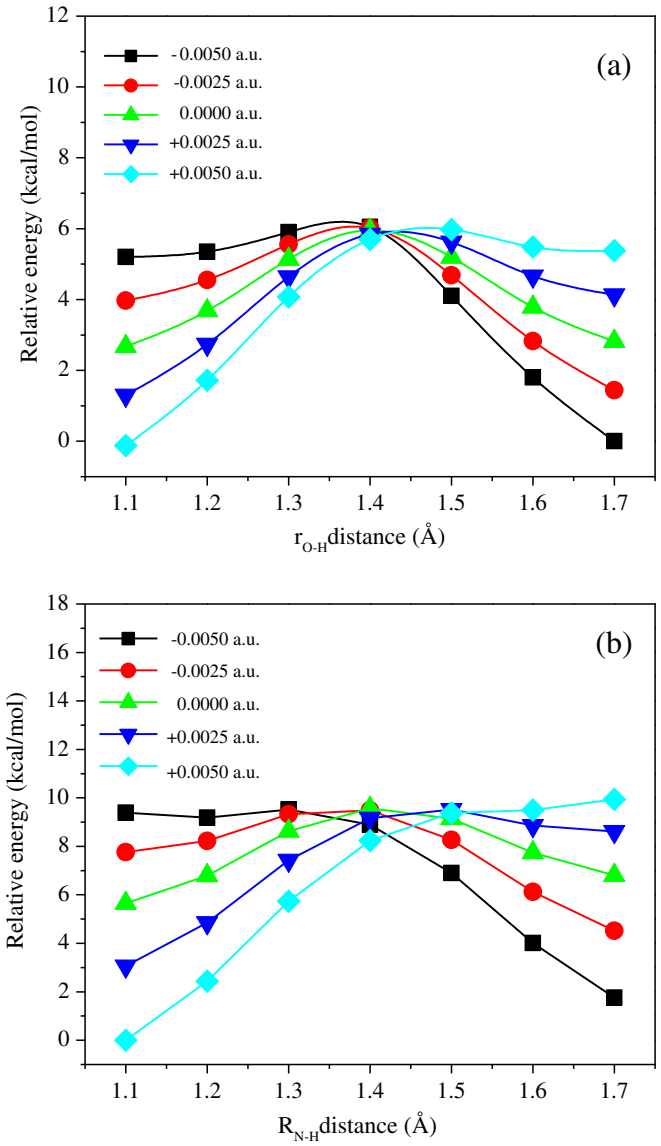

Fig. 5. Electric field effect on proton hopping in the (a) $(H_2O)H^+\cdots H_2O$ and (b) (Im)$H^+\cdots$Im systems.

Based on a review the numerous studies using atomistic simulation to achieve the molecular design of water-free proton-conducting materials, the energy profile corresponding to the molecular reorientation in an electric force field has not yet been sufficiently clarified and is usually excluded. An electric field effect on proton transfer in a water system was studied using a B3PW91/6-311++G** calculation in the gas phase by Li et al. [26]. An external electric field in the range of $\pm 5.14 \times 10^6$ to $\pm 10.28 \times 10^7$ V cm^{-1} (0.001–0.020 a.u.) was applied along the proton transfer path. When the electric field was applied opposite to the system dipole, the activation barrier for proton transport was reduced significantly. However, this study did not include dynamicity in the system to investigate the atomistic oscillation and explicit inter-atomic displacements. To fully and explicitly investigate these phenomena, density functional molecular dynamics (DFT-MD) simulations will be used to assess the electric field effect on the proton transferability of water and imidazole systems prior to the further application of this concept to more complicated imidazole-based material design.

2. Methodology

2.1. Proton transfer models for water and imidazole: isolated systems

In this study, the hydronium ion (H_3O^+) and imidazolium ion (ImH^+) were used as the proton donors in the water and imidazole systems, respectively. As the simplest models to reflect the effect of an external electric field on proton transferability, a pair of water molecules ($H_3O^+\cdots H_2O^+$) and a pair of imidazole rings ($ImH^+\cdots$Im) were employed here in the first step, as shown in Fig. 1. The models were optimised using the BLYP functional of the generalised gradient approximation (GGA) in the DMol3 module of Materials Studio version 5.5 [27]. The proton transfers in these isolated systems were investigated by a variation of the inter-molecular distance (Fig. 1(c)) in the potential energy calculation. The energy barrier change due to the reorientation of molecules was explored by the PES calculations at different inter-molecular torsional angles of $(H_2O)H^+\cdots H_2O$ (Φ) and $(Im)H^+\cdots Im$ (Ψ), as shown in Fig. 1(d). The electric field effect on proton transfer was studied by the application of the electric field along the Z direction with field strengths of ± 0.0025 a.u. (1.29×10^7 V cm^{-1}) and ± 0.0050 a.u. (2.57×10^7 V cm^{-1}) and comparison with those without an electric field. The proton transfer direction and applied electric fields are shown in Fig. 2.

2.2. Proton transfer models for water and imidazole: macroscopic phase models

Sixty water molecules and one H_3O^+ molecule were randomly arranged in a $9.00 \times 9.00 \times 22.54$ Å^3 virtual box with a density of 1 g cm^{-3}. The lowest energy structures of ten different energy configurations were chosen using the COMPASS force field. The thus-obtained structures were optimised using the BLYP functional of the GGA approximation in the Dmol^3 module. The energetically minimised structure of the water box is shown in Fig. 3a.

The bulk structure model of imidazole molecules was created as an imidazole crystal superlattice [28] of $7.58 \times 5.37 \times 29.37$ Å^3. One hydrogen ion (H^+) was added to form an ImH^+ ion. Before performing the MD simulation, the system was optimised in the same way as described for the water system. The optimised model of imidazole is shown in Fig. 3b.

2.3. MD simulations

DFT-based MD simulations were carried out to investigate the proton hopping in these systems. The BLYP functional of the GGA approximation was used, and the canonical ensemble using the Nosé–Hoover thermostat [29] was applied in the dynamics simulation. Time steps of 1.0 fs were used for the 5.0 ps simulation at 298 K. The electric field effect on proton transfer was investigated by the application of electric fields along the Z dimension with a field strength of ± 0.0025 a.u. (1.29×10^7 V cm^{-1}) and ± 0.0050 a.u. (2.57×10^7 V cm^{-1}) in comparison with those without an applied electric field.

3. Results and discussion

3.1. Proton transfer and inter-molecular reorientation in the $(H_2O)H^+\cdots H_2O$ model

The effect of intermolecular distance on the proton transfer between a pair of water molecules was studied by calculating the change in the energy barrier as a function of r_{O-O} in a PES plot (Fig. 4a). The energy barrier decreased with decreasing r_{O-O} distance. The barrier reached zero when the r_{O-O} reached a critical

distance of 2.50 Å, corresponding to r_{O-O} in a Zundel ion ($H_5O_2^+$). A sharp change in the energy barrier was found at r_{O-O} of approximately 2.7 Å, indicating behaviour differences between the two types of structures in the region.

For a fixed r_{O-O} distance, the potential energy was calculated as a function of the twisting angle Φ, as shown in Fig. 4a. The twisting angle between a pair of water molecules was varied from −180° to 180° in 30° steps. Symmetric energy profiles were achieved, and the lowest energy structure was found for the "twisted-pair" with a $|\Phi|$ of 90°. When the intermolecular distance changed by a mere 0.40 Å, significant increase in the energy barrier was observed, almost 1 kcal mol^{-1}. This finding indicates that molecular rotation during the proton transfer process is difficult. In other words, the preferred reorientation is acquired prior to the proton transfer.

An electric field was applied to investigate the effect on the proton transfer between the $(H_2O)H^+\cdots H_2O$ pair-structure. The change of the energy profiles was investigated at r_{O-O} of 2.80 Å and Φ of 90°. In this model, the proton ion was initially placed on the right side in Fig. 2. As shown in Fig. 5a, the successive change of the applied electric field gradually destroys the symmetry of the potential energy profile. The energy barrier of the system gradually decreases with a change in the applied electric field from +0.0050 to −0.0050 a.u. The application of external force in an anti-parallel direction slows the hopping, whereas a parallel electric field accelerates the proton movement by increasing the energy of the reactant while stabilising product created by the profile change accomplishing proton hopping with the lowered energy barrier.

3.2. Dynamics of hydronium ions in the proton transfer process

The study was extended to the bulk phase to include the consequences of long-distance interactions and to observe the

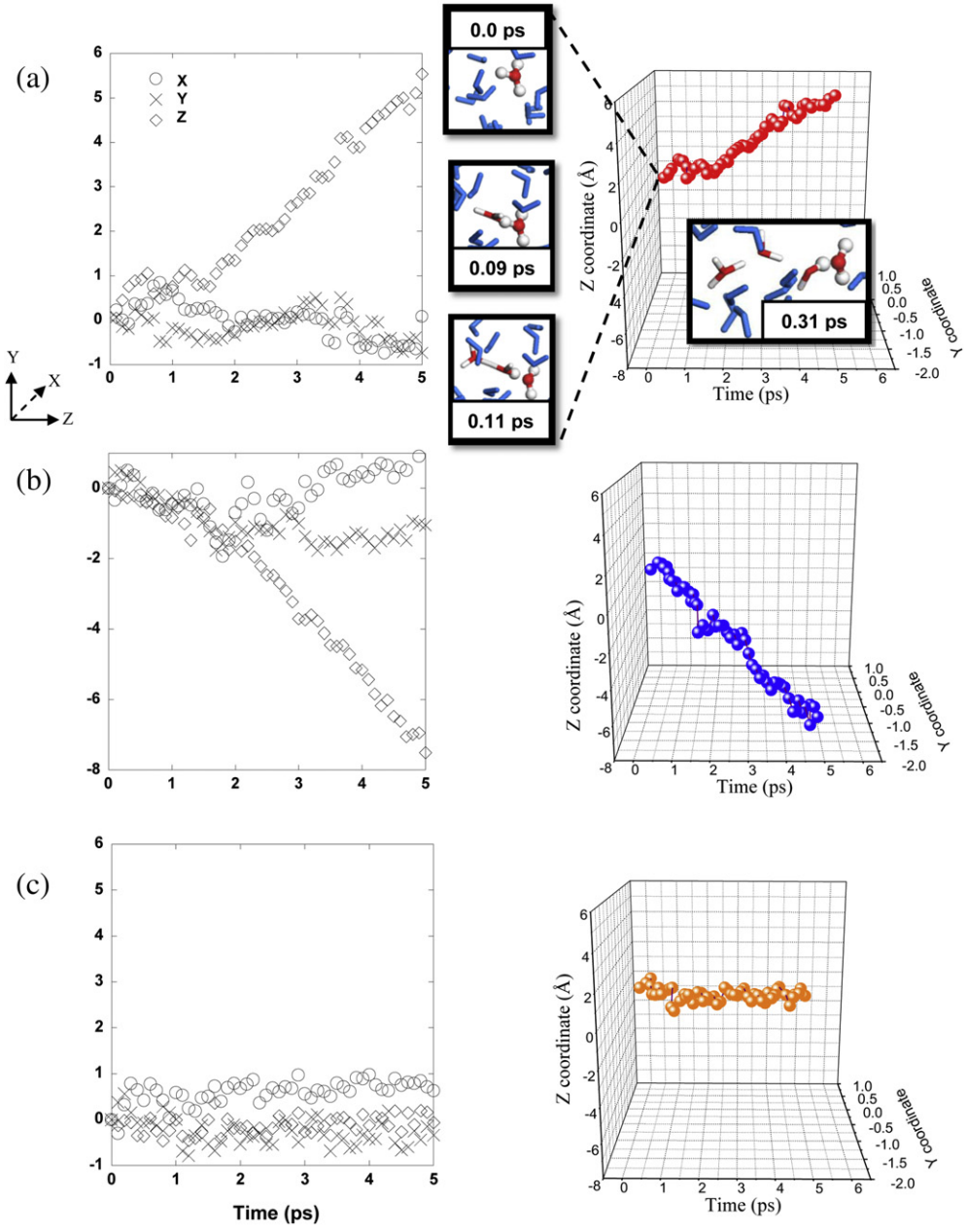

Fig. 6. Trajectory plots of H1 in the water system: (a) applied electric field of +0.0050 a.u., (b) applied electric field of −0.0050 a.u., and (c) no electric field.

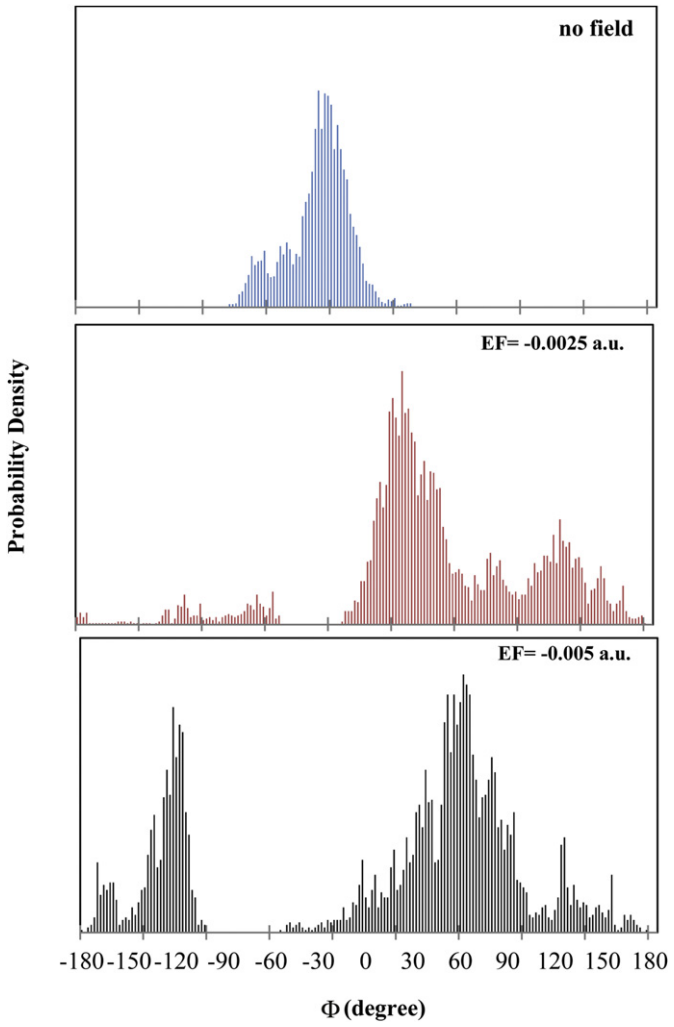

Fig. 7. Distribution of the inter-molecular torsional angle (Φ) of $(H_2O)H^+\cdots H_2O$ in the bulk model retrieved from DFT-MD simulations.

proton movement. Proton hopping in a water system was observed in the DFT-based MD simulations. The trajectory of the proton H1 confirms that the electric field controls the proton movement direction, as shown in the trajectory plots of H1 in the water system along each direction: *x*, *y*, and *z* (Fig. 6). As shown in Fig. 6c, without external electrostatic field perturbation, the proton is quite stable in its initial position. On the other hand, directional change along *z* direction was found in the applied field systems, as shown in Fig. 6a and c. Thus, the direction of the hopping process was immediately driven by the external electrostatic pole. The snapshots of proton transfer with time including the hydronium ion formation process for the systems under an applied electric field of 0.0050 a.u. are shown in Fig. 6a.

The rotational motion of water molecules during the proton transfer was investigated by DFT-MD simulations. From the DFT-MD trajectory file, the formations of the Zundel ion ($H_5O_2^+$) were observed prior to a proton transferring from the proton donor to its acceptor. During this process, the molecular orientation was examined by the calculation of the Φ torsional angle, as shown in Fig. 7. As a stronger external electrostatic field was applied to the system, the fluctuation of Φ in the dynamics increased.

To examine the efficiency of the proton conductivity, the proton diffusion coefficient was calculated using the Einstein diffusion equation [5,27,30]. The average diffusion coefficients of the H

Table 1
Proton diffusion coefficient of $(H_2O)H^+\cdots H_2O$ system with and without external electric field effect.

Electric field (a.u.)	Average diffusion coefficient $D = \frac{1(r_t - r_0)^2}{6\Delta t}$ (Å^2 ps^{-1})
0.0000	0.176
−0.0025	2.452
−0.0050	3.513
Experiment [31]	0.230

hopping in the $(H_2O)H^+\cdots H_2O$ system are shown in Table 1 both with and without the external electric field effect. When the electric field was increased from −0.0025 a.u. to −0.0050 a.u., the average diffusion coefficient increased by factors of 14 and 20, respectively.

3.3. Proton transfer and molecular reorientation in the $(Im)H^+\cdots Im$ model

A similar investigation was performed for the $(Im)H^+\cdots Im$ system. The change in the potential energy of imidazole as a function of r_{N-N} alteration was essentially the same as that for the water system (Fig. 4b). The barrier increased to 15 kcal mol^{-1} at an r_{N-N} distance of 3.00 Å. The barrier of the proton transfer process in the isolated system was zero at an r_{N-N} of 2.50 Å, which was almost the same as that for the case of $(H_2O)H^+\cdots H_2O$. By decreasing r_{N-N}, a gradual change of energy barrier was observed. At a constant r_{N-N} of 2.60 Å, the potential energy was calculated as a function of Ψ; the preferred orientation of a pair of imidazoles in the proton transfer process was found at a Ψ of 90°.

To investigate the influence of the electrostatic field, density functional calculations were performed for the preferred orientation using a Ψ of 90° under the applied electric fields from +0.0050 to −0.0050 a.u. The effect of the field on imidazole (Fig. 5b) is different from that of the $(H_2O)H^+\cdots H_2O$ system. Systematic changes in the external electrostatic field alter the energy barrier in increments, and the profile indicates that the reaction coordinates of the transition state change in this case and that reaction barrier completely disappears under an electric field of 0.0050 a.u.

3.4. Proton transfer dynamics in the $(Im)H^+\cdots Im$ superstructure

The defect in the structure was introduced by the addition of an imidazolium ion (the molecule labelled 'I' in Fig. 3b) in the superstructure of the imidazole crystal. The proton transfer of imidazole in the bulk phase was investigated from the DFT-MD trajectory of this defect-containing imidazole superlattice. The proton diffusion coefficients of the unperturbed system and those under applied electric fields of −0.0050 a.u. and −0.0075 a.u. are shown in Table 2. The proton diffusion coefficient increased by factors of 20 and 24 under the application of applied electric fields of −0.0050 a.u. and −0.0075 a.u., respectively. In this regard, the proton diffusion coefficient in the bulk phase of water and imidazole can be perturbed by an external electrostatic potential to the same degree.

Table 2
Proton diffusion coefficient of proton in $(Im)H^+\cdots Im$ superlattice analysed from DFT-MD simulations.

Electric field (a.u.)	Average diffusion coefficient $D = \frac{1(r_t - r_0)^2}{6\Delta t}$ (Å^2 ps^{-1})
0.0000	0.106
−0.0050	2.123
−0.0075	2.520

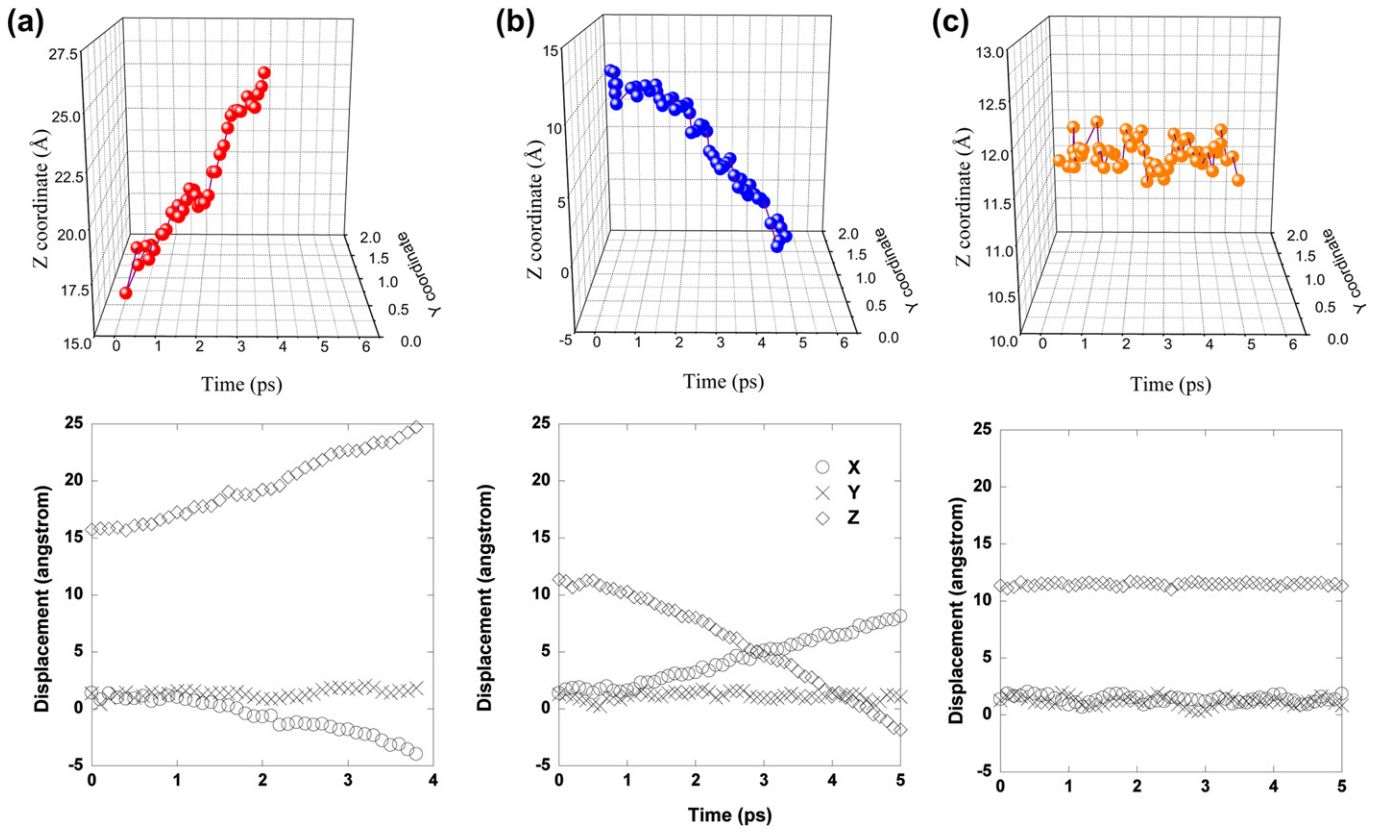

Fig. 8. Trajectory plots of H1 in the imidazole superstructure: (a) applied electric field of +0.0050 a.u., (b) applied electric field of −0.0050 a.u., and (c) no electric field.

According to the 6 ps proton trajectory (Fig. 8), the proton in the imidazole superlattice with a directional hydrogen bond in the packing could move up to 10 Å in the applied field direction. This distance is much higher than that in the system without field perturbation, which the proton moves within 2 Å of its original position. Interestingly, a rather tilted proton hopping direction was clearly indicated in the applied field system. As shown in Fig. 8a and b, a systematic change in the proton transfer along *x* and *z*

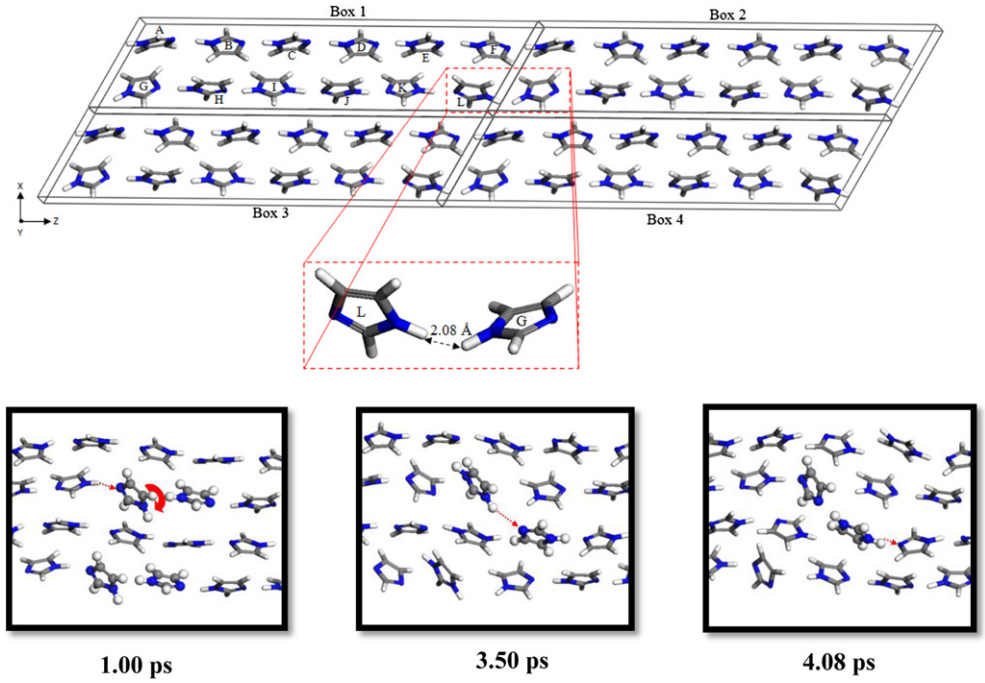

Fig. 9. Snapshots from the DFTMD trajectory of the imidazole superstructure under an external electric field of 0.0050 a.u.

directions was observed from MD trajectory. From the trajectory, after the L molecule receives a proton from the K molecule, the formed $(Im)H^+$ rotated prior to forming a bridge with the A molecule in a tilted direction (Fig. 9). This successive rotation of $(Im)H^+$ during proton transfer results in a tilted proton hopping direction, which supports the molecular reorientation suggested by previous works [19,21]. In addition, as suggested by Tashiro et al. [12] and Chirachanchai et al. [32,33], the observed phenomenon from DFT-MD simulations affirms that the designed structure incorporating imidazole to the membrane should be in well balanced of hydrogen bond network and chain mobility.

4. Conclusions

The effect of a relevant driving force from an electrostatic field was investigated in $(H_2O)H^+\cdots H_2O$, $(Im)H^+\cdots Im$, bulk water, and imidazole superlattice systems. In all cases, the electric field applied opposite to the system dipole can lead to a significant reduction of the activation barrier for proton transport processes. In the isolated systems, $(H_2O)H^+\cdots H_2O$ and $(Im)H^+\cdots Im$, the preferred intermolecular twisting angle was found at 90°. From DFT-MD simulations of the bulk system, the perturbation of applied electric fields in the range of 0.0025–0.0075 a.u. increased the proton diffusion coefficient in both water and imidazole by a factor of 14–24 times. To trace the path of proton transfer efficiency, proton movement trajectory was analysed. The directional hydrogen bond in the packing of imidazole was found to guide the proton transfer and encourage successive hopping. The reorientation of the $(Im)H^+$ molecule during proton hopping led to a tilted proton hopping direction in imidazole crystal.

Acknowledgements

The work was supported by the Thailand Research Fund (TRF), the Thailand Center of Excellence in Physics (ThEP), the Thailand Graduate Institute of Science and Technology (TGIST), the Centre for Innovation in Chemistry (PERCH-CIC), and the National Research University Project under Thailand's Office of the Higher Education Commission, Thailand.

References

[1] B. Smitha, S. Sridhar, A.A. Khan, J. Membr. Sci. 259 (2005) 10–26.
[2] P. Costamagna, S. Srinivasan, J. Power Sources 102 (2001) 242–252.
[3] M. Rikukawa, K. Sanui, Prog. Polym. Sci. 25 (2000) 1463–1502.
[4] R. Gosalawit, S. Chirachanchai, H. Manuspiya, E. Traversa, Catal. Today 118 (2006) 259–265.
[5] J. Yana, P. Nimmanpipug, S. Chirachanchai, R. Gosalawit, S. Dokmaisrijan, S. Vannarat, T. Vilaithong, V.S. Lee, Polymer 51 (2010) 4632–4638.
[6] M. Schuster, W.H. Meyer, G. Wegner, H.G. Herz, M. Ise, K.D. Kreuer, J. Maier, Solid State Ionics 145 (2001) 85–92.
[7] K.D. Kreuer, A. Fuchs, M. Ise, M. Spaeth, J. Maier, Electrochim. Acta 43 (1998) 1281–1288.
[8] K.D. Kreuer, Solid State Ionics 97 (1997) 1–15.
[9] K.D. Kreuer, Solid State Ionics 94 (1997) 55–62.
[10] N. Agmon, Chem. Phys. Lett. 244 (1995) 456–462.
[11] K.D. Kreuer, S. Adams, W. Münch, A. Fuchs, U. Klock, J. Maier, Solid State Ionics 145 (2001) 295–306.
[12] A. Pangon, P. Totsatitpaisan, P. Eiamlamai, K. Hasegawa, M. Yamasaki, K. Tashiro, S. Chirachanchai, J. Power Sources 196 (2011) 6144–6152.
[13] W.-Q. Deng, V. Molinero, W.A. Goddard, J. Am. Chem. Soc. 126 (2004) 15644–15645.
[14] P. Winget, T. Clark, J. Comput. Chem. 25 (2004) 725–733.
[15] A.D. Becke, J. Chem. Phys. 98 (1993) 1372–1377.
[16] A.D. Becke, J. Chem. Phys. 98 (1993) 5648–5652.
[17] A.D. Becke, J. Chem. Phys. 97 (1992) 9173–9177.
[18] S.J. Paddison, K.-D. Kreuer, J. Maier, Phys. Chem. Chem. Phys 8 (2006) 4530–4542.
[19] W. Münch, K.D. Kreuer, W. Silvestri, J. Maier, G. Seifert, Solid State Ionics 145 (2001) 437–443.
[20] G. Will, Z. Kristallogr. 129 (1969) 211–221.
[21] M. Iannuzzi, M. Parrinello, Phys. Rev. Lett. 93 (2004) 025901.
[22] A. Laio, M. Parrinello, Proc. Natl. Acad. Sci. U.S.A. 99 (2002) 12562–12566.
[23] M. Iannuzzi, A. Laio, M. Parrinello, Phys. Rev. Lett. 90 (2003) 238302.
[24] M. Iannuzzi, J. Chem. Phys. 124 (2006) 204710.
[25] C. Lee, W. Yang, R.G. Parr, Phys. Rev. B 37 (1988) 785–789.
[26] T. Li, A. Wlaschin, P.B. Balbuena, Ind. Eng. Chem. Res. 40 (2001) 4789–4800.
[27] Materials Studio, Accelrys Software Inc, 2011.
[28] R. Goddard, O. Heinemann, C. Kruger, Acta Crystallogr. C53 (1997) 1846–1850.
[29] M.E. Tuckerman, Y. Liu, G. Ciccotti, G.J. Martyna, J. Chem. Phys. 115 (2001) 1678–1702.
[30] M.P. Allen, D.J. Tildesley, Computer Simulation of Liquids, Oxford University Press, Oxford, 1987.
[31] A. Glättli, X. Daura, W.F. Van Gunsteren, J. Comput. Chem. 24 (2003) 1087–1096.
[32] A. Pangon, S. Chirachanchai, Polymer 53 (2012) 3878–3884.
[33] M. Jithunsa, K. Tashiro, S. Chirachanchai, Solid State Ionics 180 (2009) 132–140.